Inhibition of Antimony Sulfide (Stibnite) Scale in Geothermal Fields.

Jasbir S. Gill[1], Ph.D., Logan Muller[2], Ph.D., and David Rodman[3], Ph.D.

Nalco, an Ecolab Company
[1]Naperville IL USA
[2]Brisbane AU
[3]Auckland New Zealand

Keywords

Antimony sulfide, Stibnite, chemical inhibitors

ABSTRACT

Fouling of different components of geothermal power production is one of the limiting factors in efficient use of the geothermal resources. Most common scales are silica, calcium carbonate, and calcium sulfate while, less common are iron, iron silicate, Ba/Sr sulfate and calcium fluoride. Sulfides of antimony and arsenic are local to some geographic areas. The latter scales are highly insoluble and depend on their oxidation state, pH and temperature. Antimony sulfide, commonly known as Stibnite is quite common in New Zealand and occurs mostly in low temperature area such as binary system heat exchangers. The paper discusses laboratory and field study on the mitigation of antimony sulfide scale by the addition of scale inhibitors.

Introduction

Antimony trisulfide, commonly known as Stibnite, formation in geothermal systems is a significant problem when it occurs but its presence is limited geographically and is not a universal foulant. Stibnite deposition seems to be pretty common in binary systems in New Zealand. The fouling occurs mostly at the heat exchangers in binary system and occasionally at the reinjection well. The antimony concentration is typically quite low and stibnite appears to precipitate quantitatively, hence the heat exchangers work like a sink for stibnite deposition and thus no further antimony is available to deposit in the injection wells. Antimony trisulfide is typically a grayish color mineral but often it is not the antimony trisulfide (stibnite) that is observed on the heat exchanger but the red-orange color of antimony pentasulfide.

Wilson, et.al. (2000) [1] published results of their study indicating a big problem at the Rotokawa and Ngawha power stations. In this publication there are several other publications cited with some disagreements on the solubility of antimony sulfide. The pH and temperature changes are the main cause of stibnite precipitation. There does not seem to be any evidence regarding the antimony going in to the steam phase. The pH change is typically the result of mixing low pH condensate with brine. Even if the brine pH is 8 and if the temperature is <100ºC, stibnite is likely to precipitate out and foul the heat exchangers. Despite the total antimony in these brines being <1-2 PPM, it causes tons of deposit on the heat exchangers resulting in loss of power production.

Dr. Brown conducted a recent study (2009) [2] for Habanero 3 well. This site has a relatively high concentration of antimony at ~3.1 PPM. According to this study the brine is supersaturated with respect to stibnite at 90 ºC for pH< 9.7 condition. Similarly, the same brine which has pH ~5.96 is supersaturated at temperature<195 ºC. Thus there is a very well defined window of operation based on pH and temperature to mitigate fouling due to stibnite without any treatment. This site has chosen to design the plant with a Clean In Place (CIP) system to enable routine cleaning of the surface equipment rather than design the plant to operate within the confines of stibnite solubility. The literature value of equilibrium solubility for antimony trisulfide (K_{sp}) is 1.6E-91[3]. So it is very obvious that antimony sulfide is highly insoluble. Just to get a perspective the K_{sp} for calcium carbonate is 4.45E-09.

Many different strategies have been tried to mitigate fouling due to antimony sulfide but a great deal of success has not been achieved. There has been the use of Soft Foam Circulating balls including balls coated with corundum. However, there is no evidence that these balls are able to clean up the deposit or mitigate the formation of deposit. Cleaning using hydrochloric acid or other strong acids produced H2S, which is not desirable.

$$6\ HCl + Sb_2S_5 \rightarrow 2\ SbCl_3 + 3\ H_2S + 2\ S$$

Much of the literature indicate that it is not even certain if the antimony as measured in the brine comes as true dissolved species or some form of very fine colloidal material; most likely it is the colloidal suspension. These particles seem to be <0.5 micron [1]. It is the view of the authors' of this paper that in such situations, threshold inhibition may not be possible. Although, one can define threshold inhibition in many different ways; theoretically, it is the measure of the soluble ions, but from a practical point of view, we will define that particles that are <0.2 microns can

be considered as part of the soluble species. This paper reports the development of new inhibitors for mitigation of antimony sulfide deposition in geothermal processes based on laboratory study and a field trial.

Experimental

Two types of laboratory studies were done to evaluate different inhibitors.

Threshold Inhibition

Initially, flask studies were performed using slightly modified synthetic brine similar to the one described earlier [4]. 5 mg/L of Sb was added to the brine and silica and calcium was reduced to 100 PPM. The pH was adjusted to 5.0. The flasks were incubated at 90 °C; after 4 hours of equilibration, the hot solution was filtered through 0.22 micron Millipore, and analyzed for antimony using ICP. Antimony sulfide precipitation (particles <0.22 microns) inhibition is calculated using the following formula:

$$\% \text{ Inhibition} = (C_E - C_O)/(C_T - C_O) \text{ X } 100$$

Where

C_O = Sb concentration with no inhibitor present

CT = Sb concentration when no precipitation occurs (Initial amount of Sb (5 mg/L) added)

CE = Sb concentration when inhibitors are present.

Dispersion

Another set of tests were done to evaluate the dispersency of the antimony sulfide. This procedure was used to determine the relative efficacy of the antimony sulfide dispersant, using in situ precipitated material in the absence and presence of the inhibitor. Percent dispersion value was calculated from the light transmittance measurement through a static colloidal suspension of precipitated antimony sulfide that has been treated with the dispersant. The experimental conditions similar to the threshold procedure were followed in the dispersion study. At the end of the four hour incubation time, each flask was shaken vigorously for 20-30 seconds and let stand for 15 minutes, except for one sample without any inhibitor (T_i blank). A 5 ml aliquot was carefully removed from the center of the each flask and the % transmittance recorded. Percent dispersion was calculated using the following formula:

$$\% \text{ Dispersion} = (T_f \text{ Blank} - T_f \text{ Sample})/ (T_f \text{ Blank} - T_i \text{ Blank}) \text{ X } 100$$

Where:

T_i Blank = % Transmittance of Blank Immediately After mixing

T_f Sample = % Transmittance with Dispersant after 15 minutes standing

T_f Blank = % Transmittance of blank After 15 minutes standing

Results and Discussion

The results from the two laboratory studies are presented in Tables 1 and 2. Table 1 shows the results of threshold evaluation of three different inhibitors. These three products represent three different classes of scale inhibitors. 5200M represents a blend of proprietary phosphonate and a copolymer, GEO903 is homopolymer, and ScaleGuard 60123 is a copolymer. All three inhibitors are low molecular weight (<20,000 average number) materials and have high anionic charge density. Traditionally, 5200M has performed better than most threshold scale inhibitors for common scales such as calcium carbonate and calcium sulfate [4,5].

Table 1. Threshold inhibition of Antimony Sulfide.

Inhibitor	Inhibitor Concentration (PPM)	% inhibition
5200M	10	56
GEO 903	5	83
ScaleGuard 60123	5	90

A standard threshold inhibitor 5200M, which mostly consists of a proprietary polyphosphonate did not perform as well as the other two polymer based products. This performance comparison is based on the authors' definition of threshold inhibition, where particles <0.2 microns are considered soluble antimony. Based on these results, it brings credence to the hypothesis that for highly insoluble salts such as antimony sulfide, certain polymers with high anionic charge density are very effective in reducing the particle size and imparting negative charge to the precipitating particles and therefore are more effective than traditional threshold inhibitors such as phosphonates. It is thus quite challenging to inhibit the formation of minerals with extremely low equilibrium solubility and for such minerals the best strategy to mitigate fouling is to accept the precipitation but modify the characteristics of the precipitated particles.

The results of the dispersion study are tabulated in Table 2.

Table 2. Dispersion of Antimony Sulfide.

Inhibitor	Inhibitor Concentration PPM	% dispersion
5200M	10	60
GEO903	5	93
ScaleGuard 60123	5	95
R-4211	5	96

These results are similar to the threshold results. Again all the polymer based materials performed better than the phosphonate blend. Based on the cost and performance, copolymer ScaleGuard 60123 was chosen for further studies at a customer site using the actual brine under dynamic conditions.

Field Trial Experiment

Based on the laboratory study we selected to further evaluate the performance of ScaleGuard 60123 to inhibit antimony sulfide deposition in geothermal brines under dynamic condition. This study was done at a power plant in New Zealand. Two identical carbon steel coils of ½" pipe were immersed in a cooling water tank (Figure 1). Brine at ~ 160ºC from the brine line feeding the

Ormat Energy Converter (OEC) units was passed through the experimental coils for 21 days. The average brine outlet temperature was ~ 80ºC for both coils during the test. Although it appears that at times the exit temperature may be considerably lower than 80ºC. Typical brine flow rates were ~ 150 L/min. The brine in coil #1 was dosed with the ScaleGuard 60123 at a dose rate of 6 ppm, while coil # 2 was a control with no treatment. At the completion of the test, the coils were removed, dried and sent to GEOKEM, an outside independent laboratory for analysis. The scale deposit was investigated using Scanning Electron Microscopy (SEM), while providing high magnification images, SEM can also provide a semi-quantitative elemental analysis of the scale deposit.

Figure 1. Positions of sampling points for both coils.

Initially, the outside surface of the coils was cleaned to remove any deposit that may contaminate the analysis. Five sections, each of 80 – 100 mm in pipe-length were then cut from each coil using a non-lubricated hacksaw. These pipe sections were labeled 1- 5 and the position of these samples are shown in Figure 1. After cutting the sections, it was noticed that the appearance of the deposit on the dosed pipe was changing with distance from the inlet, and so an extra sample (#2A) was cut from this pipe midway between sample points #2 and #3. Consequently, the separate samples were labeled with the coil number first followed by the sample number as depicted in Figure 1. Thus sample "24" is from sample point 4 on coil #2 (untreated); sample 12A is sample 2A on coil # 1 (treated).

Although as previously mentioned that the brine entered the coil at 160 ºC and left at a composite temperature of 80 ºC, there were occasional losses of control over flow and temperature that would result in the system operating for unknown periods at a temperature much lower than 80 ºC. During the upset conditions, the skin temperature of the steel coil was more like 45 -50 ºC in the latter parts of the coil (e.g. 4 and 5). Given the highly temperature dependent nature of the stibnite solubility, this may be the reason why Sb deposition occurred in the treated coil. The flow was laminar thru the coils so the "exit temperature" of the brine from the coils is not representative of the temperature that the deposits were forming on the tube.

We realize that in the actual process such low temperatures will never be reached, thus this test needs to be repeated with more realistic temperature. This will require a better control on the cooling water temperature and its flow. These results will be published in the future. During the initial analysis we immediately noticed that the deposit formed in the treated coil was predominantly Silica but has a very different appearance than that of the untreated coils viz white vs. grey. As shown below in figures 2 and 3.

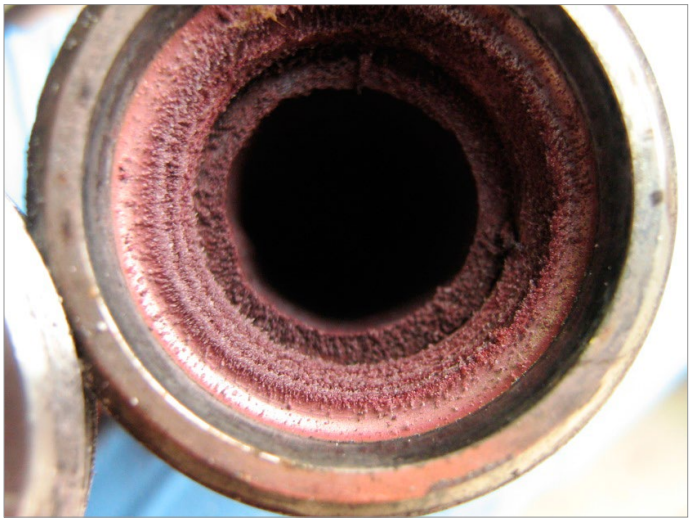

Figure 2. End coupling of the heat exchanger without the treatment.

Figure 3. End coupling of the heat exchanger with the treatment.

Most of the deposit on the untreated end coupling (Figure 2) of the heat exchanger was grey color, a typical of stibnite, while on the treated coupling it was small amount of silica, antimony and may be antimony sulfide pentahydrate. The results of the trial were quite unexpected, as there was substantial deposit formed in the treated coil compared to the untreated coil, the majority of which was silica (Figure 4) and the antimony deposit (Figure 5) was delayed compared to the control test. It is also worth noting that while in the control coil most of the antimony was in the form of traditional greyish antimony sulfide but in the treated coil, anatomy was largely present as antimony. The brine composition was such that at the low temperature it became supersaturated with respect to both silica and antimony sulfide. At the downstream end of each pipe sample, a test sample was cut with an internal pipe area of ~ 7 – 10 mm square. These samples were mounted on an aluminum stub for investigation by scanning electron microscopy (SEM). This instrument can produce images of the surface at very high magnification. It also has the capability of analyzing the chemical components of the surface by using energy dispersive x-ray analysis (EDX).

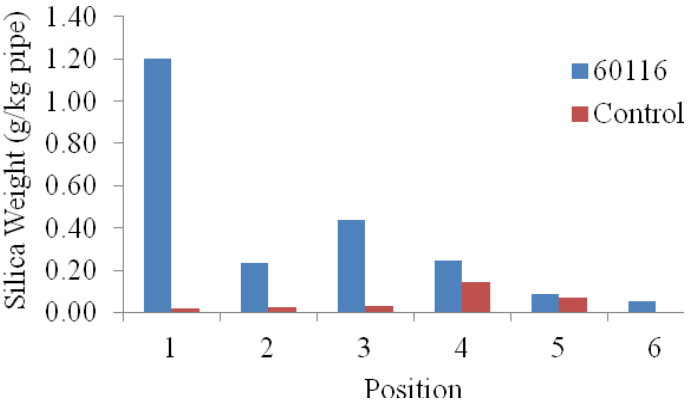

Figure 4. Weight of silica deposit along the length of the heat exchanger coil.

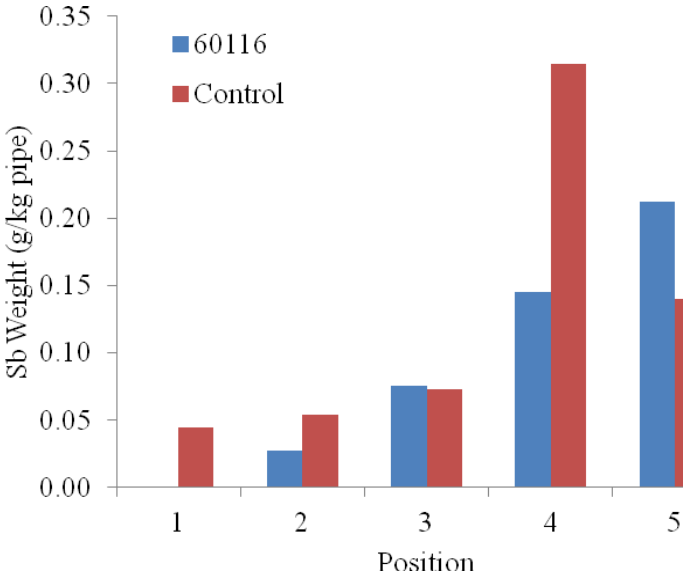

Figure 5. Weight of antimony deposit along the length of the heat exchanger coil.

The brine composition was such that at the low temperature made it supersaturated with respect to both silica and antimony sulfide. At the downstream end of each pipe sample, a test sample was cut with an internal pipe area of ~ 7 – 10 mm square. These samples were mounted on an aluminum stub for investigation by scanning electron microscopy (SEM). This instrument can produce images of the surface at very high magnification. It also has the capability of analyzing the chemical components of the surface by using energy dispersive x-ray analysis (EDX).

The approximate distance along the pipe between the centers of the sample points was measured and ranged from 60-130 cms. There were total of 5 samples and both ends of the heat exchanger were also photographed. As a representative, for discussion the sample 14 (Figure 6) showed a distinct color change from previous samples. The sample appeared to have a rusty color over the entire length of the sample. The rust color is apparent in the split pipe sample. The deposit is still soft, and there appears to be a deposit typical of colloidal silica close to the weld – possibly a result of hydrodynamic factors.

Figure 6. Sample 14 (untreated position 4) pipe section.

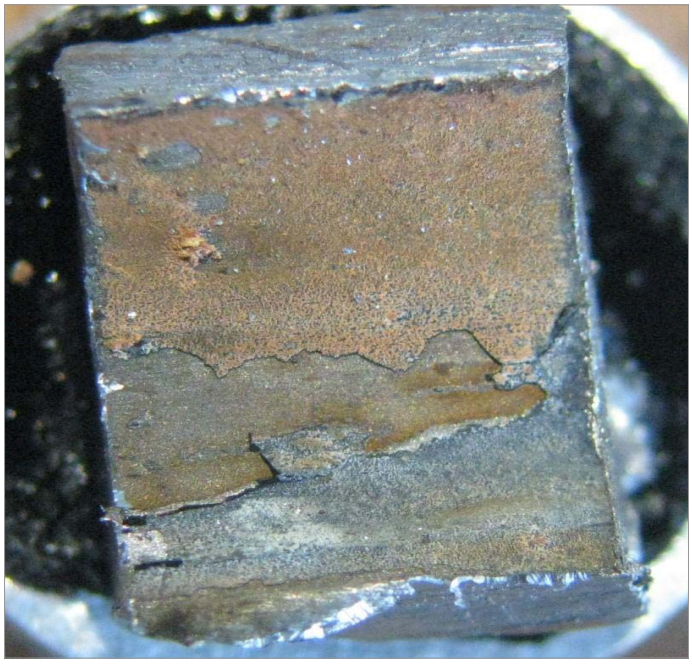

Figure 7. Optical microscope image of SEM sample 14. This sample is 7 x 8.5 mm. Fluid flow is from left to right.

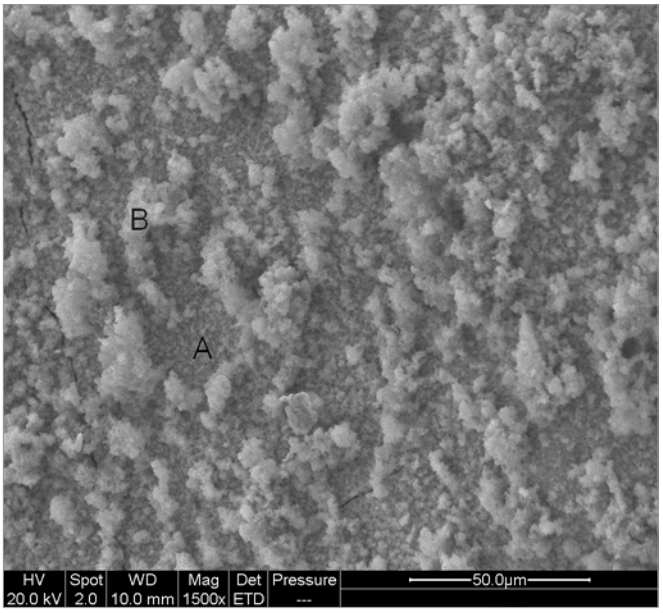

Figure 8. SEM Micrograph of sample 14.

The sample prepared for SEM analysis showed that some of the scale had come away from the steel pipe surface during preparation (Figure 7). This would indicate that the adhesion to the pipe surface is not great.

The SEM image (Figure 8) shows small colloids on top of a scale matrix. The underlying matrix shows thermal cracking due to the cooling. The colloidal material on top of the underlying scale contains more silica, whereas the underlying cemented continuous scale is mainly stibnite or elemental antimony and iron in a silica matrix.

The EDX analysis of areas A and B in Figure 8, together with a general background average EDX analysis gave the following concentrations (Table 3) when normalized to Si, S, Sb and Fe concentrations:

Table 3. Normalized to Si, S, Sb and Fe concentrations.

Element	Wt. % General	Wt.% A	Wt.%
Si	26.5	12.5	23.9
S	10.1	5.9	11.5
Sb	42.1	51.0	51.5
Fe	21.3	30.5	13.5

The significant observations from the EDX and surface analysis are:

- Silica is deposited and proportionately decreases with decreasing temperature
- Calcium is deposited in all but the final sample
- Antimony is initially deposited at low concentrations, but increases in concentration with decreasing temperature
- Although the antimony might initially be deposited as Sb2S3, it is later deposited, at least partially, as elemental antimony
- For some reason, a large concentration of iron was deposited in samples 13 and 14 – as is also obvious from the color of the deposit
- Arsenic sulfide is deposited at the lowest temperature
- Organic carbon was also detected, perhaps from the scale inhibitor

Similar study was done with the samples from the untreated coil. Figure 9 shows an optical microscope image of sample 24 (untreated position 2) which is equivalent sample position of 14 for the treated coil.

Comparison of Figures 7 and 9 shows remarkable difference in appearance of the deposit. Figure 7 (treated coil) shows a much softer-flaky deposit, while Figure 9 shows very tightly bound deposit.

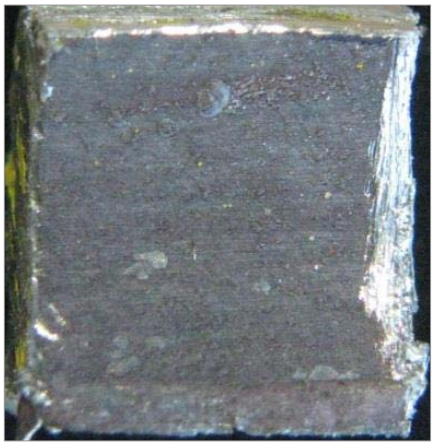

Figure 9. Optical microscope image of SEM sample 24. This sample is 7 x 8.5 mm. Fluid flow is from left to right.

There is a definite difference between the treated and untreated coils. The scales on the untreated coils consist principally of colloidal silica and colloidal antimony sulfide. As the temperature is decreased in the flowing brine, more antimony sulfide and less silica is deposited. No carbon containing deposit is found and no calcium is deposited. The antimony is probably present as amorphous antimony (III) sulfide (Sb_2S_3). Arsenic sulfide starts to deposit at the lowest temperatures. The amount of material deposited is less than that deposited in the samples from the treated coil.

The scales on the treated coils show a range of colors and compositions. All of these samples contained carbon, which probably originates from the scale inhibitor, which may have been caused by overdosing and indicates a variable to be adjusted in future tests. The overdosing was a result of plant trips and operator adjustments resulting in 50 ppm + dose rates. Silica concentrations decrease proportionately with decreasing temperature, perhaps due to exhaustion of silica concentration. Antimony is initially deposited at low concentrations, but increases with decreasing temperature, and the antimony is at least partially deposited as elemental antimony, rather than antimony sulfide.

Conclusions

There were several lessons learned from this study. The field test is part one of a series of field experiments to determine variables, metrics and to establish proof of performance. The initial phase of this study has shown that the scale inhibitor impacts the formation of antimony sulfide. Next phase is to reduce the noise from identified variables and rerun the study. Variables that impact the reliability of this type of field test were more accurately determined. For example, formation of arsenic sulfide indicates that lower temperatures were achieved in the test rig than would be found in the binary plant. Significant variables that will be better controlled in future tests include the ratio and

type of dilution water used for diluting the product, the ratio of this dilution water to the total flow and the impact of other chemical constituents introduced, temperature control in the coils, and prevention of overdosing and accurate measurement of flows through the coils. The addition of silica inhibitor such as GEO980 [6] will also improve the performance of antimony sulfide scale inhibitor.

Acknowledgements

The authors like to thank Dr. Kevin Brown of GEOKEM Barrington, Christchurch 8244, NZ kevin@geokem.co.nz for his guidance and analysis of the metal samples. The authors also like to thank Nalco an Ecolab company for permission to publish the data.

References

1. Wilson N., J. Webster-Brown, and K. Brown, 2007. "Controls on stibnite precipitation at two New Zealand geothermal power stations." Geothermics, v. 36(4), p. 330-347.
2. Brown K., 2009. "A report prepared for Geodynamics on antimony sulfide scaling" Published by Geodynamics (http://www.ga.gov.au/image_cache/GA20053.pdf).
3. Smith R.M., and A.E. Martel, 1976 "Critical stability constants." v.4, p. 77.
4. Gill J.S., 2008. "Scale Control in Geothermal Brines—New Inhibitors for Calcium Carbonate and Silica Control." GRC transactions, v. 32, p. 207-212.
5. Gill, J.S., 1996. "Development of scale inhibitors.", Corrosion 96, Paper#229.
6. Gill, J.S., and G.T. Jacobs, 2011. "Development of New Silica inhibitor – Laboratory and Field Study." GRC Transactions, v.35, p. 1243-1247.